Tracking the Contents of Spatial Working Memory during an Acute Bout of Aerobic Exercise

Jordan Garrett, Tom Bullock, and Barry Giesbrecht

Abstract

■ Recent studies have reported enhanced visual responses during acute bouts of physical exercise, suggesting that sensory systems may become more sensitive during active exploration of the environment. This raises the possibility that exercise may also modulate brain activity associated with other cognitive functions, like visual working memory, that rely on patterns of activity that persist beyond the initial sensory evoked response. Here, we investigated whether the neural coding of an object location held in memory is modulated by an acute bout of aerobic exercise. Participants performed a spatial change detection task while seated on a stationary bike at rest and during low-intensity cycling (~50 watts/50 RPM). Brain activity was measured with EEG. An inverted encoding modeling technique was employed to estimate location-selective channel response functions from topographical patterns of alpha-band (8–12 Hz) activity. There was strong evidence of robust spatially selective responses during stimulus presentation and retention periods both at rest and during exercise. During retention, the spatial selectivity of these responses decreased in the exercise condition relative to rest. A temporal generalization analysis indicated that models trained on one time period could be used to reconstruct the remembered locations at other time periods, however, generalization was degraded during exercise. Together, these results demonstrate that it is possible to reconstruct the contents of working memory at rest and during exercise, but that exercise can result in degraded responses, which contrasts with the enhancements observed in early sensory processing. ■

INTRODUCTION

Nonhuman animals and invertebrates show robust response gain in sensory processing areas during locomotion when compared to rest (Kaneko, Fu, & Stryker, 2017; Fu et al., 2014; Ayaz, Saleem, Schölvinck, & Carandini, 2013; Polack, Friedman, & Golshani, 2013; Keller, Bonhoeffer, & Hübener, 2012; Maimon, Straw, & Dickinson, 2010; Niell & Stryker, 2010). More recently, EEG studies suggest that a similar enhancement in human sensory responses may occur during bouts of acute physical exercise (Cao & Händel, 2019; Bullock, Elliott, Serences, & Giesbrecht, 2017; Bullock, Cecotti, & Giesbrecht, 2015). If sensory processes are impacted during bouts of acute aerobic exercise, then this raises the possibility that higher-order cognitive functions relying on input from these sensory areas may also be affected. Here, we test whether neural representations of object locations stored in visual working memory (WM) in humans are modulated during a bout of acute exercise.

WM is an essential cognitive process that is critical for maintaining and manipulating information. Serving as the core interface between multiple cognitive systems (e.g., learning, attention, perception, long-term memory), this process provides a platform for guiding goal-directed behaviors. Previous research has produced mixed evidence regarding modulations in WM during exercise. For instance, meta-analytic results indicate that information processing speed (i.e., reaction time) in WM tasks is enhanced during cycling, while accuracy is diminished (McMorris, Sproule, Turner, & Hale, 2011). McMorris et al. proposed that this pattern does not reflect a speed-accuracy tradeoff, but rather is because of increased peripheral and serum levels of neurotransmitters, which, in turn, engenders greater levels of neural noise in some cortical regions while facilitating activity in others. Contrary to findings that suggest WM is impaired during exercise, there is evidence that moderate intensity exercise boosts the functioning of WM overall (Martins, Kavussanu, Willoughby, & Ring, 2013). Furthermore, it has been shown that walking at a preferred speed compared to a seated rest condition can result in enhanced performance under high memory loads (Schaefer, Lövdén, Wieckhorst, & Lindenberger, 2010). Finally, concurrent exercise also has been found to have no impact on WM (Lambourne, Audiffren, & Tomporowski, 2010). Given the multimodal nature of WM (e.g., verbal, visuospatial, auditory), the heterogeneity of these findings may stem from exercise differentially affecting each domain. Indeed, there is evidence for a greater improvement of visuospatial WM compared to verbal-auditory WM as a result of exercise (Roig, Nordbrandt, Geertsen, & Nielsen, 2013). Regardless of the mixed behavioral outcomes, none of these studies provide insight into whether the underlying neural correlates of WM representations are modulated during exercise.

To investigate whether WM representations are modulated during exercise, in this study, participants performed

University of California, Santa Barbara

Journal of Cognitive Neuroscience 33:7, pp. 1271–1286
https://doi.org/10.1162/jocn_a_01714

a visuospatial change detection task at rest and during a bout of low-intensity cycling exercise while EEG was recorded at the scalp. Each trial of this task involved remembering the location of a single memorandum presented at a pseudorandomized location on the circumference of an imaginary circle centered on fixation. After a delay period (1750 msec), a test stimulus was presented at the same location or at a different location and the participant indicated whether the location of the test stimulus changed relative to the location of the memorandum presented at the beginning of the trial. Previous studies have shown that patterns of EEG alpha power (~8–12 Hz) measured at the scalp covary with the locations of attended and remembered stimuli (MacLean, Bullock, & Giesbrecht, 2019; Rihs, Michel, & Thut, 2007; Thut, Nietzel, Brandt, & Pascual-Leone, 2006; Sauseng et al., 2005), implicating a key role for this oscillation in spatial attention and WM. Here, alpha power was modeled using a computational technique, known as an inverted encoding model (IEM), to estimate the location-selective representations of the remembered locations from the unique patterns of brain activity recorded during this task. The IEM technique has been applied to fMRI BOLD activity in visual and parietal cortex (Sprague, Saproo, & Serences, 2015; Brouwer & Heeger, 2009, 2011, 2013; Serences & Saproo, 2012) as well as in scalp-recorded EEG (Samaha, Sprague, & Postle, 2016; Garcia, Srinivasan, & Serences, 2013) to recover feature- or location-selective information from the patterns coded in brain activity. Previous studies have applied this technique to patterns of scalp-recorded oscillatory activity in the alpha frequency band to successfully track the locations of items that are stored and maintained in WM with high temporal precision (MacLean et al., 2019; Sutterer, Foster, Serences, Vogel, & Awh, 2019; Foster, Sutterer, Serences, Vogel, & Awh, 2016). In addition, previous studies not only demonstrate that EEG is well suited to recording brain activity from physically active human participants (Cheron et al., 2016; Bullock et al., 2015), but also that the IEM technique can be applied effectively to the EEG steady-state visually evoked response recorded during cycling (Bullock et al., 2017). Here, the IEM technique was used to reconstruct spatially selective response profiles from topographical patterns of alpha-band activity recorded at rest and during exercise. Replicating previous work, the IEM technique revealed evidence for location-specific reconstructions of item locations held in WM coded in alpha activity at rest. Importantly, evidence for location-specific information was also observed during exercise for much of the retention period. Direct comparisons of the IEM reconstructions between rest and exercise revealed evidence for degraded representations during exercise, but only late in the retention interval.

Table 1. Demographic Information

Demographics	
Measure	*Mean ± SD*
Age (years)	21.85 ± 0.55
Height (in.)	67.79 ± 0.63
Weight (lb)	152.67 ± 4.47

METHODS

Participants

Thirty-four ($n = 34$, 17 women; see Table 1) adult student volunteers from the University of California, Santa Barbara, community took part in the study in exchange for financial compensation ($20/hr). All participants completed the Physical Activity Readiness Questionnaire (National Academy of Sports Medicine) to determine their eligibility to participate in aerobic activity. Informed consent was provided before the study began. All participants reported normal or corrected-to-normal vision. The procedures detailed below were approved by the University of California, Santa Barbara, Human Subjects Committee and the US Army Human Research Protection Office.

Visual Stimuli

Participants performed a delayed spatial change detection task (Figure 1A) to measure WM performance (Foster et al., 2016; Zhang & Luck, 2008; Wilken & Ma, 2004). A gray target circle (subtending 1.6° visual angle) served as the sample stimulus and appeared centered on a point in an imaginary circle circumventing 4° from a blue fixation dot (subtending 0.2° visual angle). The sample stimulus was presented within one of eight equally spaced 45° location bins relative to fixation (0°, 45°, 90°, 135°, 180°, 225°, 270°, 315°), with stimulus location jittered randomly within each bin between +1° and 44°. The task was presented on a 28-in. monitor (ASUS VG278Q, 1920 × 1080) via custom scripts that used functions from Psychophysics ToolBox for MATLAB (Brainard, 1997). The viewing distance was ~100 cm.

Eye-Tracking

Gaze-contingent eye-tracking was employed to ensure participants remained fixated throughout the trial period, and to minimize contamination from ocular artifacts in the EEG signal. Furthermore, this ensured a stable projection of the visual display on the retina. The eye-tracker (Eyelink 1000, SR Research Ltd.) was positioned 50–70 cm from both eyes, and binocular tracking sampling at 500 Hz was enabled. Pupil area and gaze position were collected throughout the trial period in both conditions. Pupil area was normalized using the following equation: $(x - x_{min})/(x_{max} - x_{min})$, where x is the area for a given time point.

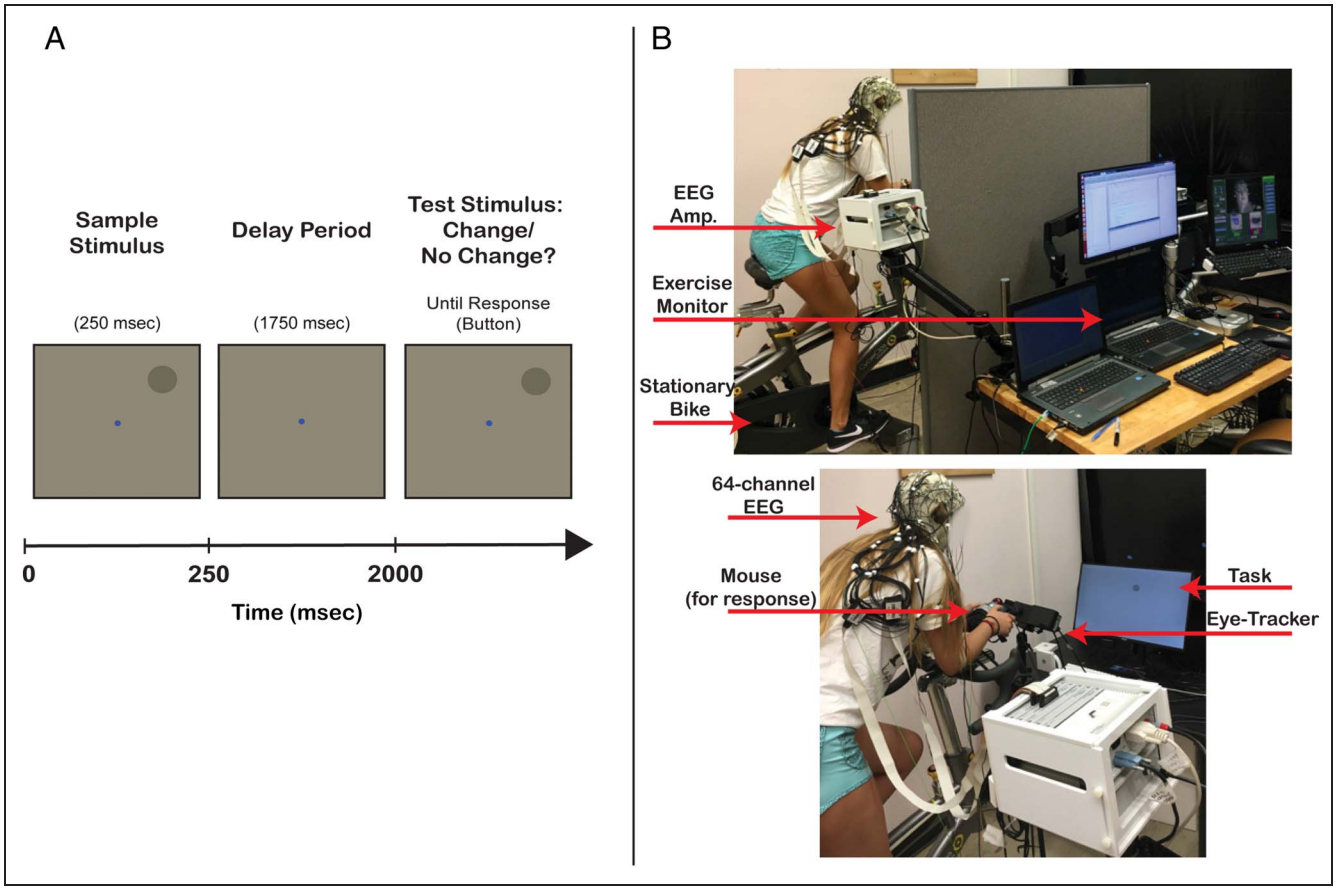

Figure 1. (A) Delayed spatial change detection task. (B) Experimental setup. Note, the task was completed in a dark room for optimal eye-tracking performance.

Stationary Bike

The stationary bike was a CycleOps 400 Pro Indoor Cycle (Saris Cycling Group). T2 + Profile Design Aero Bars (Profile Design) were attached to the handlebars, and a Logitech Trackball Mouse (Logitech) was fixed to the end of the bars (Figure 1B). The addition of the aero bars served two important purposes. First, the participant was able to lean their elbows onto the bars leaving their hands free to respond to the task. Second, the bars stabilized the participant and helped reduce head and body movement, which is a critical factor for reducing noise during EEG recording. To minimize discomfort, the bike saddle and handlebar positions were carefully adjusted for each participant. Heart rate was tracked using a CycleOps wireless heart rate monitor, whereas pedaling resistance and cadence were set and recorded through Trainer Road software (Trainer Road).

EEG

EEG data were recorded using a Brain Products ActiCHamp system (Brain Vision LLC) consisting of 64 active electrodes arranged in an actiCAP elastic cap and placed in accordance to the 10–20 System. The TP9 and TP10 electrodes were adhered directly to the right and left mastoids. Connections were established between electrodes and the scalp using SuperVisc gel (Brain Products), which is especially viscous, thus mitigating the potential for loss of signal because of gel dispersion as well as the potential for electrodes bridging because of increased sweating during exercise. At the beginning of each investigation, all impedances were reduced to below 15 kΩ. Data were sampled at 1000 Hz and referenced off-line to the average mastoid signal.

Procedure

Participants were informed of the study's structure and the intensity at which they would be required to exercise. They then completed a brief set of practice trials while cycling to ensure that they were capable of completing the task and to assess the stability of the eye-tracker. Participants were also familiarized with the Rating of Perceived Exertion (RPE) scale (Borg, 1970). RPE is a subjective rating of the intensity of physical sensations experienced during physical activity; the scale ranges from 6 (*no exertion*) to 20 (*maximal exertion*).

Prior to mounting the stationary bike, the wireless heart rate monitor and EEG cap were placed on the participant. Once on the bike, the seat position was carefully adjusted to maximize participant comfort. When ready, participants

initiated the spatial change detection task. Each trial began with the fixation dot in the center of the screen, along with a green dot (subtending 0.4° visual angle) representing the location of the participant's gaze. The participant aligned their gaze dot with the fixation dot and pressed the mouse button with their right thumb to start the trial. The fixation dot immediately turned gray to indicate that the trial was underway. The sample stimulus was then presented for 250 msec (with onset jittered randomly between 600 and 1500 msec after trial initiation). Stimulus offset was followed by a 1750-msec retention interval, where the fixation cross exclusively remained on screen. During the fixation, stimulus presentation, and retention periods, participants were instructed to maintain their gaze at the center of the screen and covertly shift attention to the position of the sample stimulus and remember its location. If gaze position deviated from fixation >2.4° or eye-blinks occurred during these periods, the trial was aborted and the message "Broken Fixation!" appeared on the screen. Aborted trials were appended to the end of the trial sequence, to ensure that a complete set of trials free from blinks and other eye movements was obtained. At the end of the retention period, a test stimulus (identical in size and color to the sample stimulus) appeared, either in the same location as the sample stimulus (50% of trials) or in a location shifted 20° clockwise or anticlockwise from the sample location (50% of trials). Participants were required to indicate whether the test stimulus appeared at the same location or different location as the sample stimulus by pressing either the left or right mouse button, respectively.

Participants completed this task in both rest and exercise conditions (counterbalanced 640 trials per exercise condition; 10 blocks of 64 trials) while seated on a stationary bike. In the exercise condition, they engaged in low-intensity cycling with a resistance of 50 watts of power and at a pedaling cadence of 50 RPM. These resistance and cadence levels were based on the intensity and cadence used in a previous study from our lab (Bullock et al., 2017). To ensure that participants maintained this cadence, they were instructed to pedal in time to a metronome set at 100 beats per minute (equaling 50 RPM). Cadence was continuously monitored throughout exercise. In the resting condition, the pedals were removed and replaced with a box positioned under each foot. Using these boxes, participants tapped their feet to a metronome set at the same frequency as described in the exercise condition, totaling 50 taps per foot per minute (equivalent to cycling cadence of 50 RPM). This manipulation was intended to attenuate possible dual-task differences between conditions that may confound modulations in WM. To mitigate any possible exercise-induced arousal carryover effects, participants who completed the exercise condition prior to the rest condition were required to sit quietly until their heart rate returned to within 10% of resting activity before beginning the resting condition.

Excluding warm-up and cool-down time, each condition took ~50 min to complete. The warm-up consisted of either cycling with the aforementioned cadence/resistance or foot tapping for 3 min. Prior to and following warm-up, the RPE scale was displayed to the participant, who then verbally reported their current level of exertion to the experimenter. Exertion ratings were also collected after every two blocks. Each experimental session took ~3.5 hr, including instrumentation time.

Biases in Eye Position

Considering that the tolerance threshold for deviations from fixation is more lenient than what is typical for studies of visual WM and attention (i.e., > 1°; Luck, 2014), it is possible that gaze position toward stimulus location may differ between rest and exercise conditions. Such an effect may be the source of differences in spatial selectivity between rest and exercise. To rule out this possibility, eye position bias was quantified by calculating the distance between fixation and stimulus location for each trial using the eye-tracking data. Distances were baseline corrected to the mean of the 200-msec prestimulus period. Because distance was computed relative to the stimulus location, more negative values would represent greater deviations toward the stimulus location. For ease of interpretation, the absolute value of the average baselined gaze position was computed and plotted in Figure 10.

EEG Preprocessing

Custom scripts in MATLAB (Version 2019a, The MathWorks Inc.) and functions from the EEGLAB toolbox (Delorme & Makeig, 2004) were used for off-line processing of the EEG data. The continuous data were referenced to the average mastoid signal and then high- and low-pass filtered between 4 and 30 Hz, respectively (EEGLAB function *pop_eegfiltnew*). The data were then resampled at 250 Hz (EEGLAB function *pop_resample*), to reduce computation time and memory demands, and epoched between −100 and 2500 sec around the onset of the stimulus. Trials that were aborted because of eye movements and trials where incorrect responses were made were excluded from any analysis. Noisy electrodes were removed via visual inspection (mean electrodes removed [mean ± *SEM*] = 1 ± 0.39). Electrodes that were excluded from one condition were also excluded from the other condition for each participant in order to avoid introducing bias when comparing EEG results across conditions. Trials exceeding ± 150 μV in remaining electrodes were then excluded (mean trials excluded overall: 4.99 ± 0.79; rest: 4.71 ± 1.28, exercise: 5.26 ± 0.95). For computing the degree of alpha lateralization (see Alpha Lateralization section below) in topographical patterns of activity at the scalp, noisy electrodes were interpolated to facilitate averaging across participants.

Spectral Decomposition

Epoched data were filtered using a third-order Butterworth bandpass filter (MATLAB function *butter*) between 8 and 12 Hz. A Hilbert transformation (MATLAB function *hilbert*) was then applied to the filtered signal in order to extract a measure of instantaneous amplitude and phase. To avoid edge artifacts, all subsequent EEG analyses were then focused on time points between −500 and 2000 msec (from 500 msec prestimulus onset to the end of the retention period). Prior to modeling, total power was calculated as the square of the absolute value of the Hilbert transformed complex values. Total power reflects continuous oscillatory activity independent of its phase relationship with stimulus onset.

Alpha Lateralization

Numerous studies have reported alpha power to be greatest over posterior electrodes ipsilateral to the cued location when compared to contralateral electrodes—indicating that spatial attention/memory alters the topographical distribution of alpha (MacLean et al., 2019; Kelly, Lalor, Reilly, & Foxe, 2006; Thut et al., 2006; Sauseng et al., 2005; Worden, Foxe, Wang, & Simpson, 2000). Furthermore, exercise has been shown to modulate power across parietal-occipital electrode sites for a range of frequencies (Ciria et al., 2019; Ciria, Perakakis, Luque-Casado, & Sanabria, 2018). Thus, the degree to which exercise influenced the systematic changes in alpha power topography was determined by normalizing (i.e., dividing) the difference in alpha power at contralateral and ipsilateral parietal/occipital electrodes sites (P5/6, P7/8, PO7/8) by the sum of power at contralateral and ipsilateral sites. Normalized alpha power at contralateral and ipsilateral sites was then averaged by condition for the stimulus (0–250 msec) and retention (500–2000 msec) time periods.

P1 ERP

Possible differences in spatial selectivity between conditions may be driven by modulations in the early visual evoked response. Considering this, the impact of exercise on the P1 ERP component was examined. Raw EEG data were first referenced to the average mastoid signal, and then high/low-pass filtered at 1 and 30 Hz, respectively. Note, this high-pass filter was applied to minimize the amount of sweat and movement related artifacts (e.g., cycling cadence was ~0.83 Hz). Afterward the data were epoched again between −500 and 2500 msec (from 500 msec prestimulus onset to the end of the retention period). Trials exceeding ± 150 μV measured at scalp electrodes of interest (P1/2, P3/4, P5/6, PO7/O8, POz/Oz, O1/2) were excluded. Three participants retained fewer than half of their trials after applying this rejection criterion, thus they were excluded only from subsequent ERP analyses. Note, we did not exclude these participants in IEM analyses because they did not yield the same amount of artifact-rejected trials when using a more aggressive high-pass filter (4 Hz), and the focus of the IEM is on WM processes rather than sensory-evoked activity. Artifact-free trials (mean overall: 494.47 ± 14.91; rest: 514.10 ± 76.46; exercise: 474.84 ± 88.12) were baseline corrected between −100 and 0 msec.

IEM

Spatially selective neural population "channel" response functions/profiles (CRFs) were estimated based on the distribution patterns of total alpha power across the scalp (Foster et al., 2016). First, the model was trained to estimate the extent to which the linear combination of a priori canonical channel responses (i.e., set of basis functions) capture the underlying structure of the observed data (topographical distribution of induced alpha power), yielding a set of regression weights. Next, these weights were tested on observed data that were excluded during training in order to estimate the channel response. The parameters of these channel response estimates were then used to quantify the spatially selective response. This method has been successfully used to reconstruct feature- and location-selective responses from human fMRI data (Ester, Sprague, & Serences, 2015; Brouwer & Heeger, 2009, 2011, 2013; Serences & Saproo, 2012; Naselaris, Kay, Nishimoto, & Gallant, 2011) and EEG recorded at the scalp (MacLean et al., 2019; Sutterer et al., 2019; Bullock et al., 2017; Foster et al., 2016; Samaha et al., 2016; Garcia et al., 2013).

The IEM was computed for each participant separately using total alpha power. Within each location bin, trials were then randomly subdivided into three samples. Note that because trial-based artifact rejection can result in an uneven number of trials per condition, it was necessary to ensure that any comparisons between conditions were not influenced by unequal trial counts. Before entering the data into the IEM, the minimum number of trials per location bin (n) was calculated across both conditions for each participant. To ensure equal numbers of trials from each location bin were entered into the model, $n-1$ trials were randomly selected from each bin. After trials were randomly subdivided into samples, these samples were then averaged. Thus, each condition included 24 samples of averaged trials (8 location bins × 3 samples of averaged trials). To ensure the outcome of the model and subsequent analyses were not influenced by an idiosyncratic selection of trials, this process was repeated 10 times, with a randomized selection of trials entered into the IEM for each of the iterations. For each iteration, an independent IEM was computed for each time point over the course of the trial (250-Hz EEG sampling rate × 2.5 sec = 625 time points) to model the temporal dynamics of the location-selective response.

For each iteration (and time point), the independent IEMs were cross-validated using a k-fold scheme, where $k = 4$. The averaged trials were randomly grouped into

four folds, with each fold having one averaged trial per location bin. Training was performed using 3/4 folds. Importantly, the IEM was trained on equivalent numbers of trials from both rest and exercise conditions to estimate a fixed encoding model. This training scheme mitigates the possibility that differences in spatial selectivity between rest and exercise are merely a reflection of differences in the signal-to-noise ratio between conditions (Gardner & Liu, 2019; Sprague, Boynton, & Serences, 2019; Liu, Cable, & Gardner, 2018; Sprague et al., 2018).

For each participant and each of the 10 iterations, IEMs were computed using the following algorithm. Let m represent the number of EEG electrodes in each data set (mean electrodes = 63 ± 0.38; equal across rest and exercise conditions within each participant), n_1 represents the number of trials in the training set (three folds of eight averaged trials), and n_2 represents the number of trials in the testing set (one fold of eight averaged trials). Let j be the number of hypothetical location-selective channels ($C_1, j \times n_1$), composed of half-sinusoidal functions raised to the seventh power as the basis set. Here, the basis set was composed of 8 equally spaced locations (i.e. $j = 8$). B_1 ($m \times n_1$) represents the training set and B_2 ($m \times n_2$) the test set. A standard implementation of the general linear model was then used to estimate the weight matrix (W, $m \times j$) using the basis set (C_1). More specifically, using the general linear model:

$$B_1 = WC_1 \tag{1}$$

Then, the ordinary least-squares estimate of W can be computed as:

$$\hat{W} = B_1 C_1^T \left(C_1 C_1^T\right)^{-1} \tag{2}$$

Using the estimated weight matrix ($\hat{W}$, Equation 2) and the test data (B_2), the channel responses C_2 ($j \times n_2$) can be estimated by:

$$\hat{C}_2 = \left(\hat{W}^T \hat{W}\right) - \hat{W}^T B_2 \tag{3}$$

After $\hat{C}_2$ was solved for each location bin, the CRF on each average trial was then circularly shifted to a common stimulus-centered reference frame (degrees of offset from channel's designated location bin), and the centered response functions were averaged across channels. The model was then repeated for each time point. The final centered CRF was computed by averaging over the 10 iterations at each time point.

IEM Generalization

To examine the temporal generalization of patterns of activity underlying spatially selective responses, IEMs were trained at each point in time, and then tested on every other point in time (ensuring independence of training and test sets). To reduce computation time (and the number of statistical comparisons), the data were down sampled to 25 Hz prior to training and testing.

Quantifying Spatially Selective Representations

Estimated channel responses were folded around 0° channel offset and transformed from (−135°, −90°, −45°, 0°, 45°, 90°, 135°, 180°) into (0°, 45°, 90°, 135°, 180°) by averaging the response at corresponding offsets (± 45°, 90°, and 135°; 0° and 180° were not averaged) for quantification. Slope was then computed (MATLAB function *polyfit*) as the linear regression weight of total alpha power across offset, and served as an index for the amount of spatial selectivity in patterns of alpha activity underlying channel responses. Larger slope values indicate greater spatial selectivity.

In addition, the IEM procedure was carried out with randomly permuted location bin labels for 250 iterations. In theory, this should generate flat channel response profiles devoid of spatial information. Slopes of these corresponding channel responses (i.e., permuted slopes) were then calculated for each iteration, which served as our null distribution for the statistical analyses of "real" slope values.

Hypothesis Testing

All statistical inference relied on computing Bayes factors (BFs) using functions from the BayesFactor toolbox for R (Morey, Rounder, & Jamil, 2015), which employs a Cauchy prior. A BF between 1 and 3 indicates "anecdotal" evidence for the alternative hypothesis, between 3 and 10 indicates "moderate" evidence, between 10 and 30 indicates "strong" evidence, and greater than 30 indicates "very strong" evidence (Kruschke & Liddell, 2018; Dienes, 2016; Wetzels et al., 2011; Kass & Raftery, 1995). BFs < 1, on the other hand, indicate varying degrees of evidence in favor of the null hypothesis (0.33–1 = anecdotal, 0.1–0.33 = moderate, 0.033–0.1 = strong, 0.01–0.033 = very strong, < 0.01 = extreme). To determine if there was evidence indicating nonzero slopes, which would be expected if the patterns of alpha contained any spatial information, one-sample BF t tests were computed using the real location labels from each trial at each time point ("real" BFs). To test for evidence indicating differences between rest and exercise conditions, paired BF t tests were used instead. The one-sample and paired-samples BF t tests were conducted for each iteration and time point using the permuted location labels, to generate a permuted distribution of BFs ("permuted" BFs) for subsequent nonparametric comparisons.

Bayesian inference is more conservative than frequentist inference, and much less likely to result in false confidence (Gelman & Tuerlinckx, 2000). Despite this, the number of statistical tests conducted overall may still be of concern, such that it may be possible to observe large BFs by chance alone. Thus, a cluster-based correction procedure (Cohen, 2014) was performed to protect against spuriously large BFs. For each iteration of permuted slopes, we calculated the maximum cluster size of contiguous time points where BF ≥ 3, resulting in a null distribution of maximum cluster sizes. For both real and permuted BFs,

only time points displaying at least moderate evidence (BF ≥ 3) in favor of the alternative hypothesis were considered for cluster-based correction. Then, the size of the real BF clusters was calculated and compared to the null distribution of cluster sizes. If a cluster was larger than 95% of the null distribution of maximum cluster sizes, it was considered to be unlikely due to chance alone.

The above statistical routine was also applied to the generalization matrix. To reduce computation time, the permutation procedure for the generalization analysis was computed for 100 iterations rather than 250 iterations.

RESULTS

Exercise Physiology

Average heart rate (Table 2) was greater during exercise (105.78 ± 3.06) as compared to rest (78.44 ± 2.66; BF > 1,000). A similar relationship was observed for mean RPE scores (BF > 1,000): rest (6.59 ± 0.11), exercise (8.65 ± 0.25). Notably, the average RPE score for the exercise condition was within the range of 9–10 on the RPE scale, which corresponds to "very light" intensity exercise. In addition, normalized pupil area was larger in the exercise condition ~1560 to 2000 msec post stimulus onset (BF ∈ [3−14], i.e., BF ranged between 3 and 14).

Behavior

Task performance was measured using sensitivity (d') and response criterion (c) (Figure 2) from signal detection theory (see Swets, 1961, for a review). Hits were defined as accurately detecting a difference between the location of sample and test stimuli. There was evidence in favor of the null hypothesis for no difference between rest and exercise conditions in the measures d' (rest: 2.23 ± 0.13, exercise: 2.27 ± 0.12; BF = 0.2) and c (rest: 0.15 ± 0.08, exercise: 0.23 ± 0.07; BF = 0.56).

Topographical Distribution of Alpha Power across the Scalp

Prior to modeling the contribution of alpha activity to WM representations, the topographical distribution of power across the scalp was examined. Qualitatively, alpha power increased over posterior electrodes ipsilateral to the presented stimulus location in the resting condition, a finding consistent with prior work (Figure 3A; MacLean et al., 2019; Kelly et al., 2006; Thut et al., 2006; Sauseng et al., 2005; Worden et al., 2000). More importantly, a similar pattern was present in the exercise condition. When analyzing the degree of alpha lateralization, there was moderate evidence in favor of the null hypothesis for no difference between conditions during both the stimulus (0–250 msec; rest: 0.06 ± 0.03, exercise: 0.04 ± 0.02; BF = 0.22) and retention (500–2000 msec; rest: 0.04 ± 0.02, exercise: 0.02 ± 0.01; BF = 0.37) periods (Figure 3B).

Table 2. Means and Standard Errors for the Physiological and Subjective Report Data

Exercise Physiology			
Condition	*Heart Rate (BPM)*	*RPE*	*Cadence (RPM)*
Rest	78.44 ± 2.66	6.59 ± 0.11	–
Exercise	105.78 ± 306	8.65 ± 0.25	54.77 ± 0.65

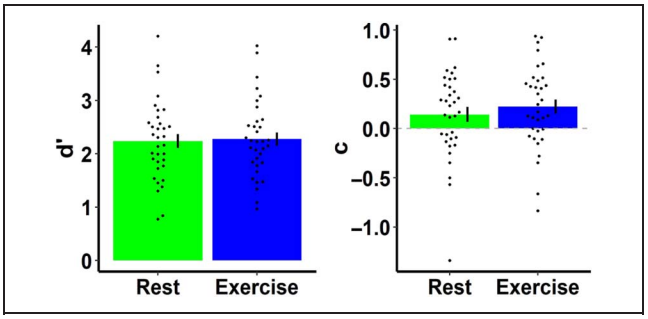

Figure 2. Working Memory task performance as measured by sensitivity (d') and response criterion (c) in both conditions. Points represent each individual's data, and error bars represent ±1 *SEM*.

Reconstructing Representations of Stimulus Location

The IEM analysis using alpha band activity yielded evidence for spatially selective responses in both conditions (Figure 4). Reconstructed response profiles reached peak amplitude ~200 msec after stimulus onset, which is consistent with previous studies using the IEM approach to track locations maintained in WM (MacLean et al., 2019; Foster et al., 2016). Comparing real slopes to their permuted null distributions revealed there was at least moderate evidence for differences throughout the encoding and retention periods in both conditions (Figure 5A; rest: BF ∈ [3, 3.55×10^9], exercise: BF ∈ [3, 2.23×10^{11}]), confirming that mental representations of remembered locations can be successfully reconstructed both at rest and during exercise. Nevertheless, there was evidence for decreases in slope between ~926–1255 msec (BF ∈ [3, 238]) and ~1643–1864 msec (BF ∈ [3, 41]) post stimulus onset during exercise compared to rest. These results suggest that, although there was evidence for a location-selective representation in alpha activity during exercise, this representation was degraded during late stages of retention (Figure 5B).

Exercise Modulates Processes Underlying Spatial Selectivity

Models trained on patterns of activity within a specific time period that can recover spatially selective responses when tested on activity from a differing time period exhibit generalization (MacLean et al., 2019; van Moorselaar et al.,

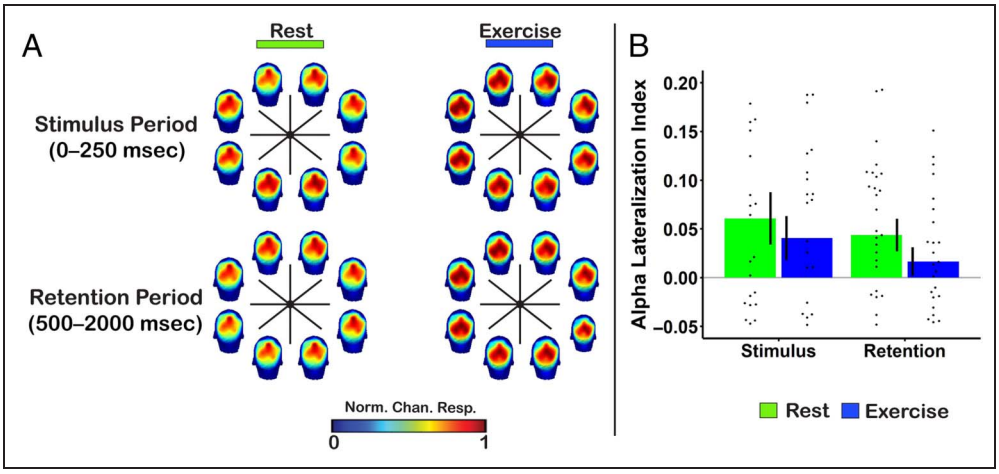

Figure 3. (A) Topographical distribution of alpha (8–12 Hz) power across the scalp during encoding and retention periods, normalized across parietal/parieto-occipital electrodes within each location bin. The location of each head plot reflects the corresponding sample stimulus location bin. Note, a time frame of 500–2000 msec was used for the retention period to avoid including stimulus evoked activity. (B) Alpha lateralization during the stimulus and retention periods as a function of exercise condition. Points represent each individual's data, and error bars represent ±1 *SEM*.

2018; King & Dehaene, 2014). Successful generalization suggests that a stable unitary code underlies a cognitive process or processes throughout time. In contrast, failure of models to generalize in this fashion implies that the trained/tested patterns of activity represent different codes. Note, a lack of generalization is not an indication that neural activity during that time period does not support representations of location in WM, given that reconstruction was successful from ~100 msec onwards when training and testing within time points.

When testing the fixed encoding model on activity in the resting condition, there was evidence for temporal generalization throughout the entire trial period poststimulus onset (Figure 6 "Test: Rest"). Strong generalization throughout time indicates that spatial selectivity at rest is supported by a stable unitary code. There was also evidence for temporal generalization during exercise, but it was degraded relative to a permuted null distribution (Figure 6 "Test: Exercise"). Comparing the degree of generalization between conditions, there was evidence for greater generalization when training on activity between ~900 and 1200 msec and testing on activity within the same time period in the resting condition (BF ∈ [3.89, 148.12]). Taken together, these results imply that similar unitary codes underlie the representation of locations in WM during both rest and exercise, but that the stability of this code over time is degraded during exercise.

Control Analyses

Differences in Reconstruction Are Not Caused by Differences in Spectral Activity

A series of control analyses were performed on spectral activity to determine any confounding factors in our observed differences of selectivity between conditions. One such analysis was the comparison of total spectral power between the rest and exercise conditions. Spectral power across a range of frequency bands has been shown to be modulated during exercise (e.g., Bullock et al., 2017; Kubitz & Mott, 1996). Thus, it is possible that the observed differences in spatial selectivity and generalization may

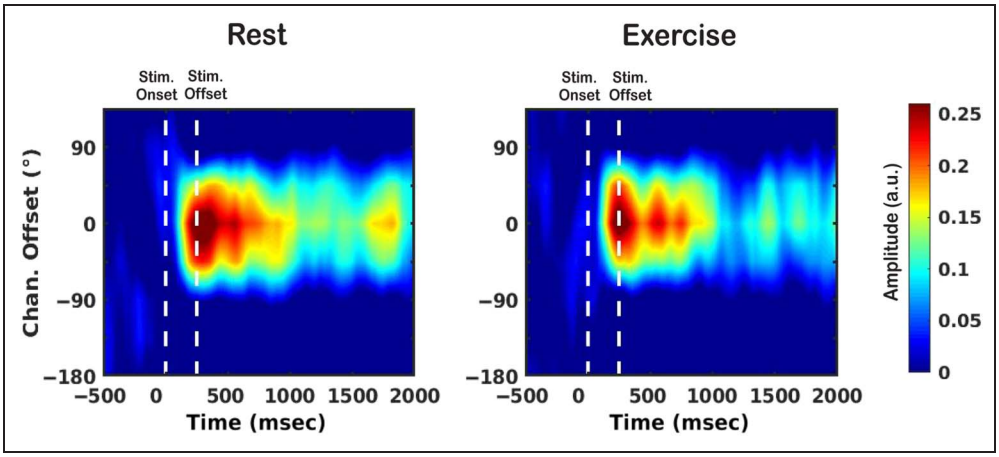

Figure 4. Estimated channel responses as a function of stimulus-centered location offset (−180°, −135°, −90°, −45°, 0°, 45°, 90°, 135°), reconstructed over time from patterns of alpha-band activity. Plotted CRFs are baseline corrected relative to the average amplitude across channels in a prestimulus window of −500 to 0 msec.

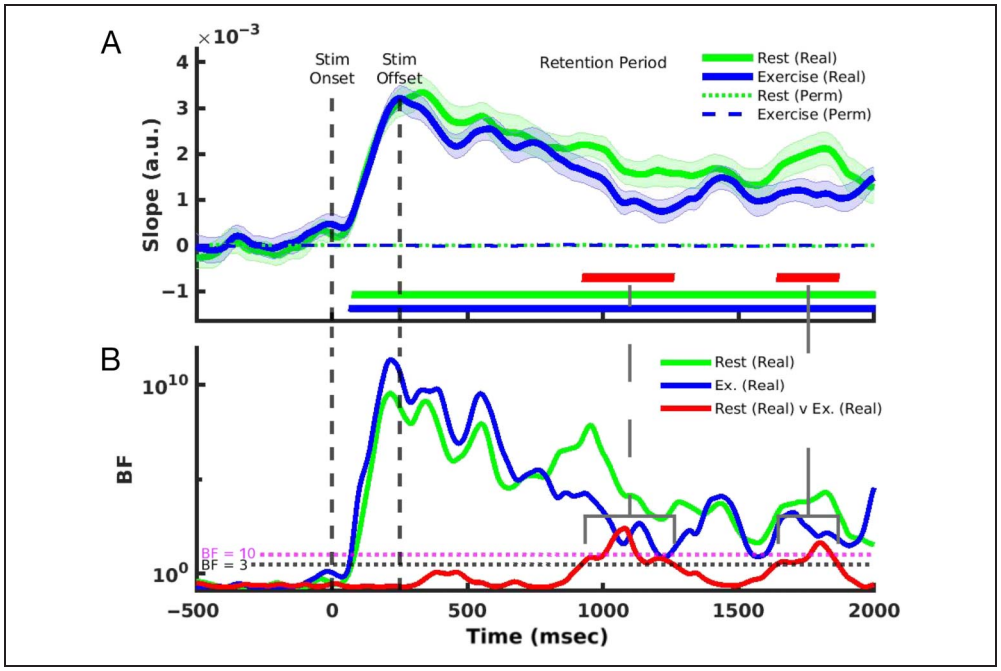

Figure 5. (A) Spatially selective CRF slopes. Horizontal green and blue bars indicate time points with at least moderate evidence for real rest and exercise slope estimates being different from zero, respectively. Horizontal red bars indicate time points with at least moderate evidence for a difference between real rest and exercise slopes. Cluster correction was applied to all comparisons, and clusters shown are those whose size exceeded 95% of a permuted null distribution. (B) BFs for comparisons made at each time point. Shaded error bars represent ± 1 *SEM*.

reflect exercised-induced fluctuations in power that are independent of WM processes. EEG data were high-pass filtered at 4 Hz, and spectral power was computed for post-stimulus neural activity (0–2000 msec) using a fast Fourier transform (MATLAB function *fft*). There was at least moderate evidence for a difference in power between the following frequency ranges: 7–7.4 Hz (BF ∈ [4.11, 5.81]), 11.4–13 Hz (BF ∈ [5.85, 1.04 × 10^3]), and ~14–30 Hz (BF ∈ 3.12, 1.51 × 10^3; Figure 7A).

Considering there was evidence for a difference between conditions in the upper range of alpha total power averaged over the trial period (~11 to 12 Hz), it is possible that fluctuations in alpha power over time may be driving decreased selectivity in the exercise condition. To assess this possibility, the time-course of mean total alpha power was compared between both conditions. There was no evidence for differences; if anything, there was evidence in favor of the null hypothesis (BF ∈ [0.18, 0.71]; Figure 7B). Importantly, this suggests that decreased spatial selectivity during exercise is a product of alterations in the topographical distribution of alpha power over time rather than dramatic changes in global alpha power.

Degraded Reconstructions Are Not Due to Location Information Being Carried by Other Frequencies during Exercise

Previous research has shown that topographical patterns of oscillatory activity outside the alpha frequency range do not track the contents of spatial WM (Foster et al.,

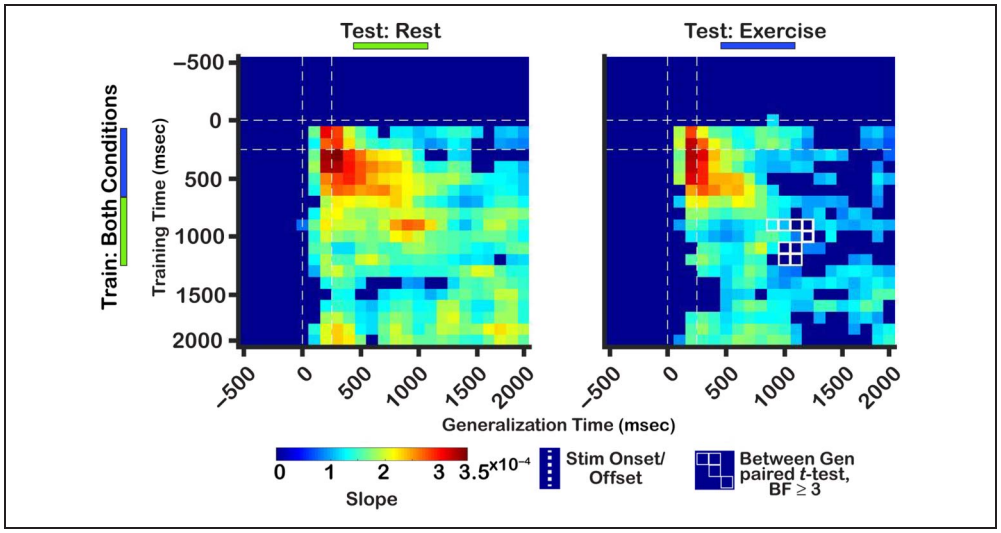

Figure 6. IEM generalizations. Only contiguous time points with at least moderate evidence for slope estimates being different from zero (cluster corrected) are shown. All other time points are in dark blue. The *y*-axis represents time points trained on, whereas the *x*-axis is time points tested on. Successful generalization to the right of the main diagonal indicates forward temporal generalization, whereas the opposite direction indicates backward temporal generalization.

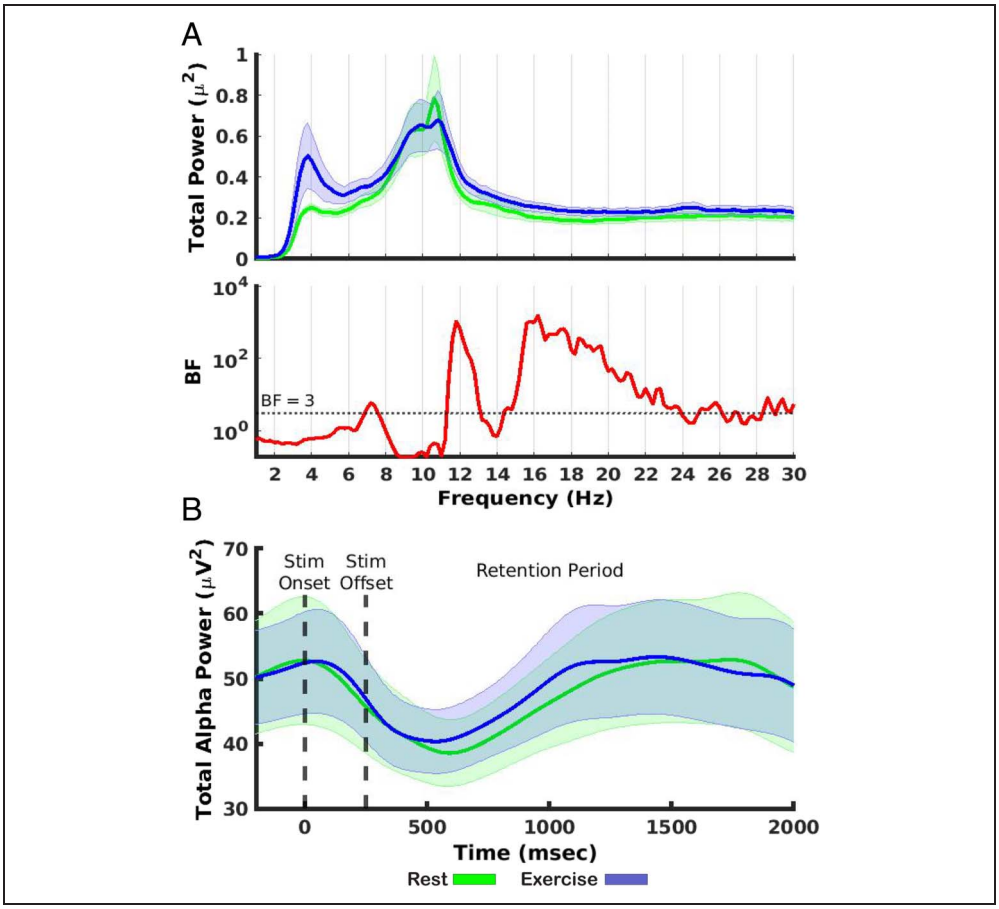

Figure 7. Control analyses on spectral activity conducted to assess the validity of IEM findings. (A) Top: Total power averaged across time for all frequency bands between 4 and 30 Hz. Peak response occurred over the alpha band range. Bottom: BF values comparing power at each frequency between rest and exercise. (B) Alpha power over time. Dashed lines indicate stimulus onset (0 msec) and stimulus offset (250 msec). Shaded error bars represent ± 1 *SEM*.

2016). Yet, it is possible that these frequency bands may be recruited during a bout of exercise. This would imply that decreases in slope amplitude in the exercise condition reflect a possible change between frequency bands that support representations. Considering this, the IEM routine was applied to total power across a broad range of frequencies (4–30 Hz in 1-Hz increments; Figure 8). When testing for nonzero slopes in the computed single frequency CRFs, at least moderate evidence in favor of the alternative hypothesis was only observed for activity within the alpha frequency band range for both rest (BF $\in$ [3, 1.86 $\times$ 10^6]) and exercise (BF $\in$ [3, 2.15 $\times$ 10^7]). Evidence in favor of differences in single frequency slopes between conditions did not survive cluster-based corrections. Thus, decreases in alpha slope amplitude in the retention period during exercise (Figure 5A) do not reflect the recruitment of

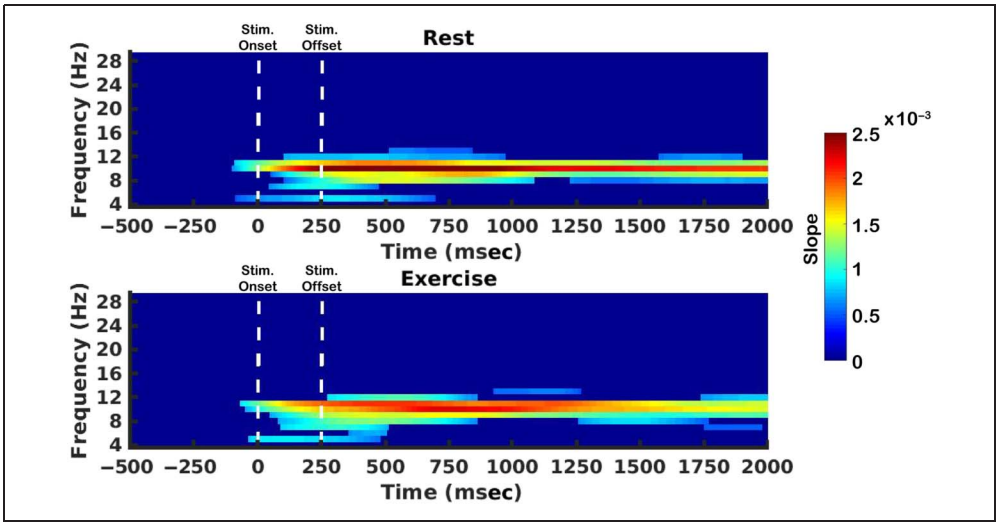

Figure 8. The IEM routine was applied to frequencies within the range of 4–30 Hz at 1-Hz increments. Shown here are the slopes of reconstructed CRFs with at least moderate evidence for being different from zero (cluster corrected). Those that were not different are colored in dark blue.

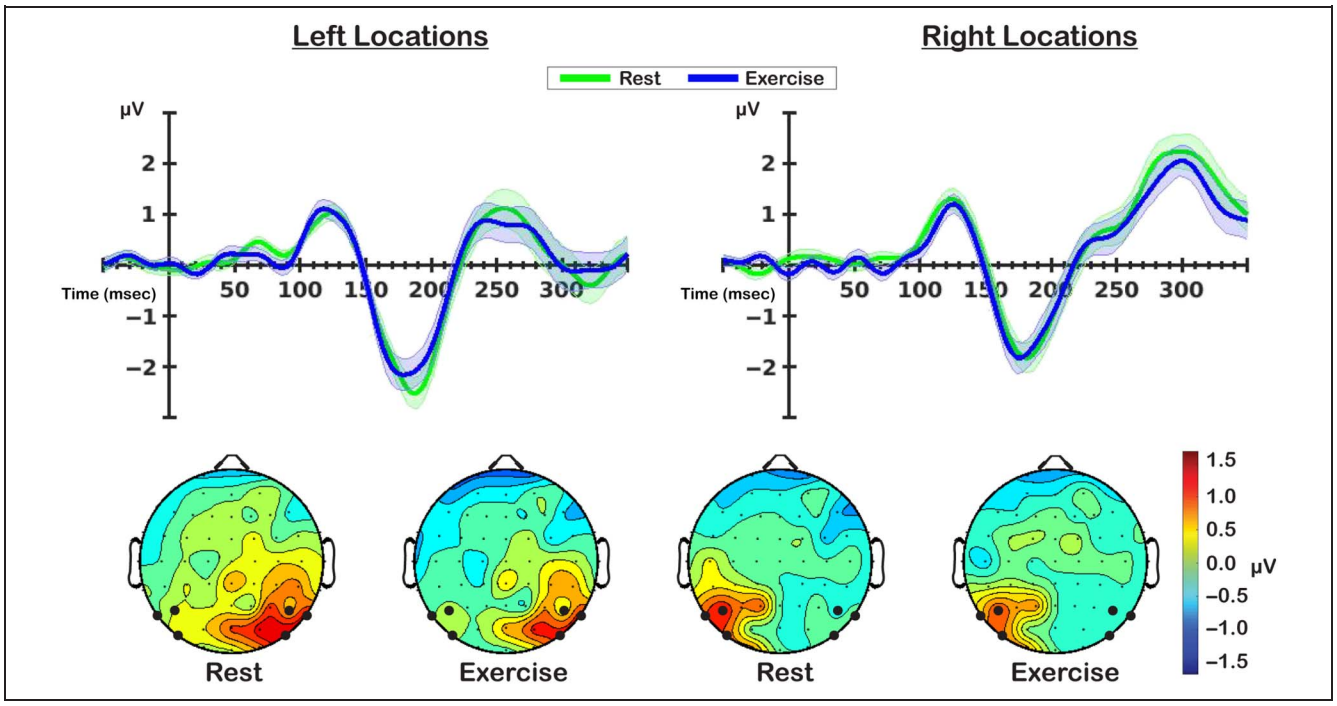

Figure 9. P1 analyses. Top plots depict P1 components for memoranda presented at left and right locations in the display. Bottom plots show topographical distribution of mean P1 amplitude between 116 and 136 msec. Electrodes colored in black represent the ones used for computation of lateralized difference ERPs.

non-alpha frequency bands to support representations of location specific information.

Visual Evoked Responses

For each location, we calculated the difference in activity between parieto-occipital electrodes (PO7/O8, P5/6, P7/8) ipsilateral to the presented stimulus locations and those that were contralateral. Then, difference waves were averaged for locations on either side of the vertical meridian, yielding two P1 components: one for left locations and the other for right locations (Figure 9). P1 mean amplitude was calculated by finding the peak latency of the positive going component between 100 and 150 msec post stimulus onset, and subsequently calculating mean amplitude ±10 msec around this peak. There was moderate evidence in favor of the null hypothesis of no difference between rest and exercise P1 mean amplitudes for left (rest: 1.19 ± 0.13, exercise: 1.3 ± 0.15; BF = 0.26) and right locations (rest: 1.49 ± 0.17, exercise: 1.44 ± 0.15; BF = 0.19). These results suggest that the observed differences in spatial selectivity are not due to modulations of the visual evoked response.

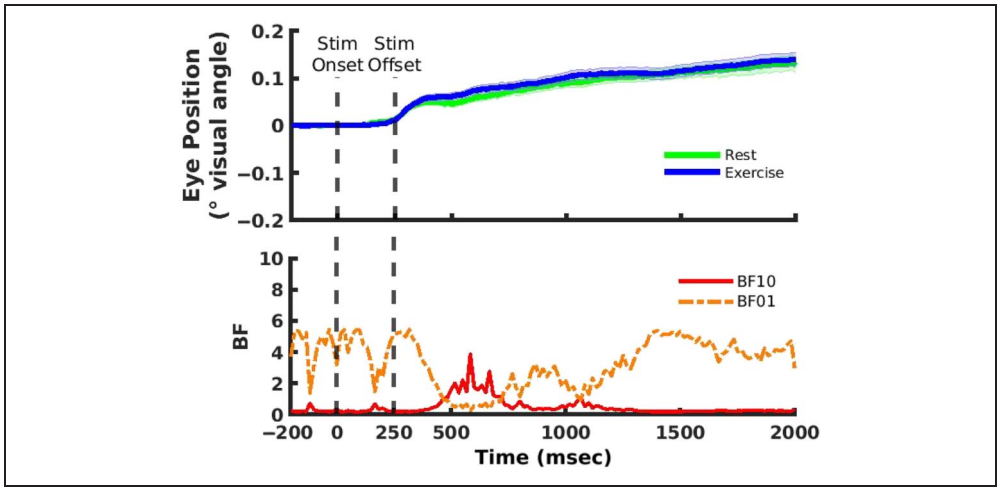

Figure 10. Top: Eye position bias (i.e., baseline corrected distance of gaze from stimulus location in units of degrees of visual angle) for both the rest and exercise conditions. Bottom: BF values for comparisons between rest and exercise. One time point at 538 msec showing at least moderate evidence in favor of the alternative hypothesis did not survive cluster correction. Shaded error bars represent ± 1 *SEM*.

Eye Position

To assess whether the difference in the spatially selective responses derived from alpha band activity is contaminated by differential eye movements toward remembered locations in the rest and exercise conditions, we compared eye position throughout the stimulus and retention periods. There was a small increase in eye position bias throughout the trial period in both conditions, but this bias toward the stimulus location did not exceed 0.15° in either condition. Moreover, point-wise comparisons did not reveal evidence for differences that survived cluster correction (Figure 10). If the cluster correction was not applied, there was a single time point that indicated moderate evidence (BF = 3.86) for a difference between rest and exercise conditions at ~538 msec poststimulus onset, but this difference was small (0.02°), occurred during a period when the slopes of the spatial reconstructions were declining, and did not occur at the same time point when evidence for differences between the slope of the spatial reconstructions in exercise and rest were observed. In contrast, there was moderate evidence in favor of the null hypothesis of no difference in eye position bias between rest and exercise at multiple time points throughout the trial period (BF $\in$ [3, 5.44]). Therefore, eye position biases were likely not the cause of decreased spatial selectivity during exercise.

DISCUSSION

Evidence from human, nonhuman animal, and invertebrate studies has demonstrated that early sensory visual processes are modulated during bouts of acute physical activity (Kaneko et al., 2017; Bullock et al., 2015, 2017; Fu et al., 2014; Ayaz et al., 2013; Pontifex & Hillman, 2007). The goal of this study was to determine whether higher-order cognitive operations that depend on these sensory responses are also impacted during physical activity. EEG was recorded from human participants while they engaged in a spatial change detection task at rest and during a bout of cycling exercise. The IEM technique was then applied to activity in the alpha band in order to reconstruct spatially selective response profiles for item locations stored in WM. There were two key results. First, in addition to replicating previous work demonstrating that topographically specific patterns of alpha band activity track the contents of WM at rest (MacLean et al., 2019; Foster et al., 2016), the present results also demonstrate that it is possible to reconstruct spatially selective response profiles during item encoding and retention while participants are engaged in a bout of physical activity. Second, although there was evidence for a spatially selective response during exercise, our results also indicate that the quality of this reconstructed location information is degraded relative to the rest condition, but only during the late stages of the retention period.

The finding that topographic patterns of total alpha activity track the specific position of a behaviorally relevant stimulus both during encoding and retention replicates a number of studies in the literature indicating that the neural populations that give rise to alpha oscillations in human EEG code information in WM in a location-selective manner (Sutterer, Polyn, & Woodman, 2021; MacLean et al., 2019; Sutterer et al., 2019; Foster et al., 2016). The results reported here also show that these location-selective codes can be reconstructed from patterns of neural activity acquired during exercise. Critically, the slopes of the location-selective profiles were greater than zero throughout the trial, indicating that the location-selective WM representations coded in alpha band activity are robust to changes in global behavioral state.

Despite the robust location-selective reconstructions during encoding and retention observed here, there was also clear evidence during the late stages of retention (> 900 msec) that the selectivity of these reconstructions was degraded during exercise relative to rest. One possible explanation for the degraded reconstructions of spatially selective response profiles is that WM representations coded in the alpha band are more fragile later in the retention period and vulnerable to decay during exercise. Another possible explanation, that is not mutually exclusive from the previous explanation, is that the rest and exercise conditions may differ in their attentional demands. The similar level of behavioral performance in the two tasks is inconsistent with this interpretation; however, the behavioral task was very easy and may thus not have been sensitive to more subtle differences in attentional demands between the two conditions. Although we took measures to equate the conditions by requiring participants to cycle to the beat of a metronome in the exercise condition and to tap their feet to the metronome in the rest condition, it is still possible that cycling to the beat of a metronome requires greater attentional control than foot tapping and interferes with attention-based rehearsal of locations in WM (Postle, Awh, Jonides, Smith, & D'Esposito, 2010; Awh et al., 1999, Awh & Jonides, 1998). Importantly, previous work has shown that shifts in attention from memoranda in WM toward an opposing task disrupt spatial selectivity (van Moorselaar et al., 2018). The notion that cycling can impact resource allocation in a concurrent cognitive task is supported by previous work demonstrating modulation of various sensory and cognitive ERP components (Bullock et al., 2015; Pontifex & Hillman, 2007; Grego et al., 2004; Yagi, Coburn, Estes, & Arruda, 1999). Future work that manipulates levels of dual-task interference between conditions (e.g., higher levels during rest) and employs a more complex WM task is necessary to elucidate the cause of decreased spatial selectivity during exercise.

Given that topographic patterns of alpha activity also track with attended locations in spatial attention tasks (Samaha et al., 2016; Rihs et al., 2007; Thut et al., 2006; Sauseng et al., 2005), it is reasonable to question whether the location-selective response profiles observed here at rest and during exercise represent WM activity or covert

spatial attention to the location of the memoranda. There is some evidence against a solely attention-based interpretation of the present results. For example, in covert attention tasks that have revealed spatially specific responses to attended locations, alpha power tends to ramp-up in amplitude prior to the attended stimulus over ipsilateral sites (Banerjee, Snyder, Molholm, & Foxe, 2011; Rihs et al., 2007). Here, however, after the initial reduction in alpha power driven by the evoked response, total alpha was relatively constant up to the presentation of the test stimulus. Furthermore, the presence of sustained delay period activity in the absence of a stimulus is a classic indicator of WM (Sreenivasan & D'Esposito, 2019; Vogel, McCollough, & Machizawa, 2005; Vogel & Machizawa, 2004). Though the quality of reconstructions degraded over time, the slopes of profiles were greater than zero throughout the entire trial period. In contrast, the profiles of reconstructions observed in spatial attention tasks increase during periods prior to target onset (Samaha et al., 2016). It is important to note that we are not arguing that spatial attention is not involved, rather we are arguing that the pattern of results is unlikely to be driven by covert attention alone. Moreover, when considering the present findings together with those in the literature providing evidence for the strong connection between spatial WM and spatial attention, our results are consistent with the notion that spatial attention facilitates the coding and maintenance of spatial representations held in WM (Oberauer, 2019; Postle et al., 2010; Awh et al., 1999, Awh & Jonides, 1998).

Previous studies have reported evidence for exercise-induced enhancements of visual processing (Bullock et al., 2015, 2017). Here, however, there was no difference in P1 mean amplitude or location selectivity between the two conditions during this period, indicating that the initial sensory coding was similar in the two conditions. These contrasting findings between our studies may be because of the considerable differences in visual stimulation, task demands, or the nature of the data submitted to an IEM. For instance, in Bullock et al. (2015), participants performed an oddball task with large stimuli presented at fixation. Bullock et al. (2017) required participants to judge orientation changes occurring in large, high contrast, centrally presented flickering grating stimuli. Furthermore, they estimated orientation-selective stimulus reconstructions using 15-Hz steady-state stimulus evoked activity. Here, participants were required to remember the location of a small, gray item presented in the periphery and location-selective reconstructions are based on induced alpha band activity. The discrepancy between the results reported here and the exercise-induced enhancements observed in previous work from our laboratory (Bullock et al., 2015, 2017) and by others (Pesce, Capranica, Tessitore, & Figura, 2003) may also reflect a difference in the effect of global physiological states on sensory evoked responses to attended stimuli (i.e., as in the previous work) and in activity that persists well beyond the sensory evoked response, such as WM retention-related activity.

Patterns of activity coding for spatial locations displayed robust generalization throughout time when testing on activity in the resting condition, indicating the presence of a stable unitary code. This pattern of generalization is consistent with previous research showing the presence of a rapid selection process that supports locations held in WM when external visual input is continuous (MacLean et al., 2019). Although generalization when testing on activity in the exercise condition was not as robust relative to the resting condition, a stable unitary code was also found to support spatial selectivity when participants are in a physically active state. Importantly, the successful reconstruction of spatially selective responses when applying the fixed IEM to activity throughout time from each condition separately suggests a common unitary code underlies the maintenance of locations in WM in both physiological states. In later stages of the retention period, this unitary code is degraded when one is concurrently engaged in exercise.

As with all simultaneous neuroimaging and exercise studies, EMG and sweat artifacts are potentially confounding factors in our results. The contribution of EMG artifacts was minimized by stabilizing each participant's position on the bike using aero bars, and coaching them to ensure they limited upper body movement during cycling or foot tapping. EMG typically occurs at higher frequencies (> 30 Hz), whereas sweat artifacts are low frequency (< 1 Hz) oscillations (Thompson, Steffert, Ros, Leach, & Gruzelier, 2008). Because the IEM analyses presented here were based on alpha power (8–12 Hz), it is unlikely that our results were seriously contaminated by these artifacts.

In summary, we used the IEM technique to investigate how spatial selectivity for locations held in WM is modulated during an acute bout of aerobic exercise when compared to rest. Reconstruction of location-selective representations was successful during both rest and exercise, but stimulus representations were degraded at specific time points during the retention period as a function of exercise. Evidence also suggested that WM representations were supported by a unitary code during both rest and exercise. The current study is the first to demonstrate that representations of items stored in WM can be reconstructed during a bout of physical exercise and provides novel insight into both the modulation and composition of these representations during exercise when compared to rest. Future research will focus on uncovering how exercise-induced degradation of stimulus representations in WM impacts behavior in the human.

Reprint requests should be sent to Jordan Garrett, Psychological & Brain Sciences, University of California Santa Barbara, 93106-9010, or via e-mail: jordan.garrett@psych.ucsb.edu.

Funding Information

This work was supported by the Institute for Collaborative Biotechnologies through cooperative agreement W911NF-

19-2-0026 with the U.S. Army Research Office. The content of the information does not necessarily reflect the position or policy of the government and no official endorsement should be inferred.

Diversity in Citation Practices

A retrospective analysis of the citations in every article published in this journal from 2010 to 2020 has revealed a persistent pattern of gender imbalance: Although the proportions of authorship teams (categorized by estimated gender identification of first author/last author) publishing in the *Journal of Cognitive Neuroscience (JoCN)* during this period were M(an)/M = .408, W(oman)/M = .335, M/W = .108, and W/W = .149, the comparable proportions for the articles that these authorship teams cited were M/M = .579, W/M = .243, M/W = .102, and W/W = .076 (Fulvio et al., *JoCN*, 33:1, pp. 3–7). Consequently, *JoCN* encourages all authors to consider gender balance explicitly when selecting which articles to cite and gives them the opportunity to report their article's gender citation balance.

REFERENCES

Ayaz, A., Saleem, A. B., Schölvinck, M. L., & Carandini, M. (2013). Locomotion controls spatial integration in mouse visual cortex. *Current Biology*, *23*, 890–894. **DOI:** https://doi.org/10.1016/j.cub.2013.04.012, **PMID:** 23664971, **PMCID:** PMC3661981

Awh, E. & Jonides, J. (1998). Spatial working memory and spatial selective attention. In R. Parasuraman (Ed.), *The attentive brain* (pp. 353–380). Cambridge, MA: MIT Press.

Awh, E., Jonides, J., Smith, E. E., Buxton, R. B., Frank, L. R., Love, T., et al., (1999). Rehearsal in spatial working memory: Evidence from neuroimaging. *Psychological Science*, *10*, 433–437. **DOI:** https://doi.org/10.1111/1467-9280.00182

Banerjee, S., Snyder, A. C., Molholm, S., & Foxe, J. J. (2011). Oscillatory alpha-band mechanisms and the deployment of spatial attention to anticipated auditory and visual target locations: Supramodal or sensory-specific control mechanisms? *Journal of Neuroscience*, *31*, 9923–9932. **DOI:** https://doi.org/10.1523/JNEUROSCI.4660-10.2011, **PMID:** 21734284, **PMCID:** PMC3343376

Borg, G. (1970). Perceived exertion as an indicator of somatic stress. *Scandinavian Journal of Rehabilitation Medicine*, *2*, 92–98. **DOI:** https://doi.org/10.1037/t58166-000, **PMID:** 5523831

Brainard, D. H. (1997). The psychophysics toolbox. *Spatial Vision*, *10*, 433–436. **DOI:** https://doi.org/10.1163/156856897X00357, **PMID:** 9176952

Brouwer, G. J., & Heeger, D. J. (2009). Decoding and reconstructing color from responses in human visual cortex. *Journal of Neuroscience*, *29*, 13992–14003. **DOI:** https://doi.org/10.1523/JNEUROSCI.3577-09.2009, **PMID:** 19890009, **PMCID:** PMC2799419

Brouwer, G. J., & Heeger, D. J. (2011). Cross-orientation suppression in human visual cortex. *Journal of Neurophysiology*, *106*, 2108–2119. **DOI:** https://doi.org/10.1152/jn.00540.2011, **PMID:** 21775720, **PMCID:** PMC3214101

Brouwer, G. J., & Heeger, D. J. (2013). Categorical clustering of the neural representation of color. *Journal of Neuroscience*, *33*, 15454–15465. **DOI:** https://doi.org/10.1523/JNEUROSCI.2472-13.2013, **PMID:** 24068814, **PMCID:** PMC3782623

Bullock, T., Cecotti, H., & Giesbrecht, B. (2015). Multiple stages of information processing are modulated during acute bouts of exercise. *Neuroscience*, *307*, 138–150. **DOI:** https://doi.org/10.1016/j.neuroscience.2015.08.046, **PMID:** 26318337

Bullock, T., Elliott, J. C., Serences, J. T., & Giesbrecht, B. (2017). Acute exercise modulates feature-selective responses in human cortex. *Journal of Cognitive Neuroscience*, *29*, 605–618. **DOI:** https://doi.org/10.1162/jocn_a_01082, **PMID:** 27897672

Cao, L., & Händel, B. (2019). Walking enhances peripheral visual processing in humans. *PLoS Biology*, *17*, e3000511. **DOI:** https://doi.org/10.1371/journal.pbio.3000511, **PMID:** 31603894, **PMCID:** PMC6808500

Cheron, G., Petit, G., Cheron, J., Leroy, A., Cebolla, A., Cevallos, C., et al. (2016). Brain oscillations in sport: Toward EEG biomarkers of performance. *Frontiers in Psychology*, *7*, 246. **DOI:** https://doi.org/10.3389/fpsyg.2016.00246

Ciria, L. F., Luque-Casado, A., Sanabria, D., Holgado, D., Ivanov, P. C., & Perakakis, P. (2019). Oscillatory brain activity during acute exercise: Tonic and transient neural response to an oddball task. *Psychophysiology*, *56*, e13326. **DOI:** https://doi.org/10.1111/psyp.13326, **PMID:** 30637763, **PMCID:** PMC7311047

Ciria, L. F., Perakakis, P., Luque-Casado, A., & Sanabria, D. (2018). Physical exercise increases overall brain oscillatory activity but does not influence inhibitory control in young adults. *Neuroimage*, *181*, 203–210. **DOI:** https://doi.org/10.1016/j.neuroimage.2018.07.009, **PMID:** 29981904

Cohen, M. X. (2014). *Analyzing neural time series data: theory and practice*. Cambridge, MA: MIT Press. **DOI:** https://doi.org/10.7551/mitpress/9609.001.0001

Delorme, A., & Makeig, S. (2004). EEGLAB: An open source toolbox for analysis of single-trial EEG dynamics including independent component analysis. *Journal of Neuroscience Methods*, *134*, 9–21. https://www.sccn.ucsd.edu/eeglab/. **DOI:** https://doi.org/10.1016/j.jneumeth.2003.10.009, **PMID:** 15102499

Dienes, Z. (2016). How Bayes factors change scientific practice. *Journal of Mathematical Psychology*, *72*, 78–89. **DOI:** https://doi.org/10.1016/j.jmp.2015.10.003

Ester, E. F., Sprague, T. C., & Serences, J. T. (2015). Parietal and frontal cortex encode stimulus-specific mnemonic representations during visual working memory. *Neuron*, *87*, 893–905. **DOI:** https://doi.org/10.1016/j.neuron.2015.07.013, **PMID:** 26257053, **PMCID:** PMC4545683

Foster, J. J., Sutterer, D. W., Serences, J. T., Vogel, E. K., & Awh, E. (2016). The topography of alpha-band activity tracks the content of spatial working memory. *Journal of Neurophysiology*, *115*, 168–177. **DOI:** https://doi.org/10.1152/jn.00860.2015, **PMID:** 26467522, **PMCID:** PMC4760461

Fu, Y., Tucciarone, J. M., Espinosa, J. S., Sheng, N., Darcy, D. P., Nicoll, R. A., et al. (2014). A cortical circuit for gain control by behavioral state. *Cell*, *156*, 1139–1152. **DOI:** https://doi.org/10.1016/j.cell.2014.01.050, **PMID:** 24630718, **PMCID:** PMC4041382

Garcia, J. O., Srinivasan, R., & Serences, J. T. (2013). Near-real-time feature-selective modulations in human cortex. *Current Biology*, *23*, 515–522. **DOI:** https://doi.org/10.1016/j.cub.2013.02.013, **PMID:** 23477721, **PMCID:** PMC3608396

Gardner, J. L., & Liu, T. (2019). Inverted encoding models reconstruct an arbitrary model response, not the stimulus. *eNeuro*, *6*. **DOI:** https://doi.org/10.1523/ENEURO.0363-18.2019, **PMID:** 30923743, **PMCID:** PMC6437661

Gelman, A., & Tuerlinckx, F. (2000). Type S error rates classical and Bayesian single and multiple comparison procedures. *Computational Statistics*, *15*, 373–390. **DOI:** https://doi.org/10.1007/s001800000040

Grego, F., Vallier, J. M., Collardeau, M., Bermon, S., Ferrari, P., Candito, M., et al. (2004). Effects of long duration exercise on cognitive function, blood glucose, and counterregulatory hormones in male cyclists. *Neuroscience Letters*, *364*, 76–80. **DOI:** https://doi.org/10.1016/j.neulet.2004.03.085, **PMID:** 15196681

Kaneko, M., Fu, Y., & Stryker, M. P. (2017). Locomotion induces stimulus-specific response enhancement in adult visual cortex. *Journal of Neuroscience*, *37*, 3532–3543. **DOI:** https://doi.org/10.1523/JNEUROSCI.3760-16.2017, **PMID:** 28258167, **PMCID:** PMC5373133

Kass, R. E., & Raftery, A. E. (1995). Bayes factors. *Journal of the American Statistical Association*, *90*, 773–795. **DOI:** https://doi.org/10.1080/01621459.1995.10476572

Keller, G. B., Bonhoeffer, T., & Hübener, M. (2012). Sensorimotor mismatch signals in primary visual cortex of the behaving mouse. *Neuron*, *74*, 809–815. **DOI:** https://doi.org/10.1016/j.neuron.2012.03.040, **PMID:** 22681686

Kelly, S. P., Lalor, E. C., Reilly, R. B., & Foxe, J. J. (2006). Increases in alpha oscillatory power reflect an active retinotopic mechanism for distracter suppression during sustained visuospatial attention. *Journal of Neurophysiology*, *95*, 3844–3851. **DOI:** https://doi.org/10.1152/jn.01234.2005, **PMID:** 16571739

King, J. R., & Dehaene, S. (2014). Characterizing the dynamics of mental representations: The temporal generalization method. *Trends in Cognitive Sciences*, *18*, 203–210. **DOI:** https://doi.org/10.1016/j.tics.2014.01.002, **PMID:** 24593982, **PMCID:** PMC5635958

Kruschke, J. K., & Liddell, T. M. (2018). The Bayesian new statistics: Hypothesis testing, estimation, meta-analysis, and power analysis from a Bayesian perspective. *Psychonomic Bulletin & Review*, *25*, 178–206. **DOI:** https://doi.org/10.3758/s13423-016-1221-4, **PMID:** 28176294

Kubitz, K. A., & Mott, A. A. (1996). EEG power spectral densities during and after cycle ergometer exercise. *Research Quarterly for Exercise and Sport*, *67*, 91–96. **DOI:** https://doi.org/10.1080/02701367.1996.10607929, **PMID:** 8735998

Lambourne, K., Audiffren, M., & Tomporowski, P. D. (2010). Effects of acute exercise on sensory and executive processing tasks. *Medicine and Science in Sports and Exercise*, *42*, 1396–1402. **DOI:** https://doi.org/10.1249/MSS.0b013e3181cbee11, **PMID:** 20019631

Liu, T., Cable, D., & Gardner, J. L. (2018). Inverted encoding models of human population response conflate noise and neural tuning width. *Journal of Neuroscience*, *38*, 398–408. **DOI:** https://doi.org/10.1523/JNEUROSCI.2453-17.2017, **PMID:** 29167406, **PMCID:** PMC5761616

Luck, S. J. (2014). *An introduction to the event-related potential technique*. Cambridge, MA: MIT Press.

MacLean, M. H., Bullock, T., & Giesbrecht, B. (2019). Dual process coding of recalled locations in human oscillatory brain activity. *Journal of Neuroscience*, *39*, 6737–6750. **DOI:** https://doi.org/10.1523/JNEUROSCI.0059-19.2019, **PMID:** 31300523, **PMCID:** PMC6703892

Maimon, G., Straw, A. D., & Dickinson, M. H. (2010). Active flight increases the gain of visual motion processing in Drosophila. *Nature Neuroscience*, *13*, 393–399. **DOI:** https://doi.org/10.1038/nn.2492, **PMID:** 20154683

Martins, Q. A., Kavussanu, M., Willoughby, A., & Ring, C. (2013). Moderate intensity exercise facilitates working memory. *Psychology of Sport and Exercise*, *14*, 323–328. **DOI:** https://doi.org/10.1016/J.PSYCHSPORT.2012.11.010

McMorris, T., Sproule, J., Turner, A., & Hale, B. J. (2011). Acute, intermediate intensity exercise, and speed and accuracy in working memory tasks: A meta-analytical comparison of effects. *Physiology and Behavior*, *102*, 421–428. **DOI:** https://doi.org/10.1016/j.physbeh.2010.12.007, **PMID:** 21163278

Morey, R. D., Rouder, J. N., & Jamil, T. (2015). Package 'BayesFactor' (R Package Version 0.9.12-2).

Naselaris, T., Kay, K. N., Nishimoto, S., & Gallant, J. L. (2011). Encoding and decoding in fMRI. *Neuroimage*, *56*, 400–410. **DOI:** https://doi.org/10.1016/j.neuroimage.2010.07.073, **PMID:** 20691790, **PMCID:** PMC3037423

Niell, C. M., & Stryker, M. P. (2010). Modulation of visual responses by behavioral state in mouse visual cortex. *Neuron*, *65*, 472–479. **DOI:** https://doi.org/10.1016/j.neuron.2010.01.033, **PMID:** 20188652, **PMCID:** PMC3184003

Oberauer, K. (2019). Working memory and attention—A conceptual analysis and review. *Journal of Cognition*, *2*, 36. **DOI:** https://doi.org/10.5334/joc.58, **PMID:** 31517246, **PMCID:** PMC6688548

Pesce, B. R., Capranica, L., Tessitore, A., & Figura, F. (2003). Focusing of visual attention under submaximal physical load. *International Journal of Sport and Exercise Psychology*, *1*, 275–295. **DOI:** https://doi.org/10.1080/1612197X.2003.9671719

Polack, P.-O., Friedman, J., & Golshani, P. (2013). Cellular mechanisms of brain state-dependent gain modulation in visual cortex. *Nature Neuroscience*, *16*, 1331–1339. **DOI:** https://doi.org/10.1038/nn.3464, **PMID:** 23872595, **PMCID:** PMC3786578

Pontifex, M. B., & Hillman, C. H. (2007). Neuroelectric and behavioral indices of interference control during acute cycling. *Clinical Neurophysiology*, *118*, 570–580. **DOI:** https://doi.org/10.1016/j.clinph.2006.09.029, **PMID:** 17095295

Postle, B. R., Awh, E., Jonides, J., Smith, E. E., & D'Esposito, M. (2010). The where and how of attention-based rehearsal in spatial working memory. *Cognitive Brain Research*, *20*, 194–205. **DOI:** https://doi.org/10.1016/j.cogbrainres.2004.02.008, **PMID:** 15183391

Rihs, T. A., Michel, C. M., & Thut, G. (2007). Mechanisms of selective inhibition in visual spatial attention are indexed by α-band EEG synchronization. *European Journal of Neuroscience*, *25*, 603–610. **DOI:** https://doi.org/10.1111/j.1460-9568.2007.05278.x, **PMID:** 17284203

Roig, M., Nordbrandt, S., Geertsen, S. S., & Nielsen, J. B. (2013). The effects of cardiovascular exercise on human memory: A review with meta-analysis. *Neuroscience and Biobehavioral Reviews*, *37*, 1645–1666. **DOI:** https://doi.org/10.1016/j.neubiorev.2013.06.012, **PMID:** 23806438

Samaha, J., Sprague, T. C., & Postle, B. R. (2016). Decoding and reconstructing the focus of spatial attention from the topography of alpha-band oscillations. *Journal of Cognitive Neuroscience*, *28*, 1090–1097. **DOI:** https://doi.org/10.1162/jocn_a_00955, **PMID:** 27003790, **PMCID:** PMC5074376

Sauseng, P., Klimesch, W., Stadler, W., Schabus, M., Doppelmayr, M., Hanslmayr, S., et al. (2005). A shift of visual spatial attention is selectively associated with human EEG alpha activity. *European Journal of Neuroscience*, *22*, 2917–2926. **DOI:** https://doi.org/10.1111/j.1460-9568.2005.04482.x, **PMID:** 16324126

Schaefer, S., Lövdén, M., Wieckhorst, B., & Lindenberger, U. (2010). Cognitive performance is improved while walking: Differences in cognitive–sensorimotor couplings between children and young adults. *European Journal of Developmental Psychology*, *7*, 371–389. **DOI:** https://doi.org/10.1080/17405620802535666

Serences, J. T., & Saproo, S. (2012). Computational advances towards linking BOLD and behavior. *Neuropsychologia*, *50*, 435–446. **DOI:** https://doi.org/10.1016/j.neuropsychologia.2011.07.013, **PMID:** 21840553, **PMCID:** PMC3384549

Sprague, T. C., Adam, K. C. S., Foster, J. J., Rahmati, M., Sutterer, D. W., & Vo, V. A. (2018). Inverted encoding models assay population-level stimulus representations, not single-unit neural tuning. *eNeuro*, *5*. **DOI:** https://doi.org/10.1523

/ENEURO.0098-18.2018, **PMID:** 29876523, **PMCID:** PMC5987635
Sprague, T. C., Boynton, G. M., & Serences, J. T. (2019). The importance of considering model choices when interpreting results in computational neuroimaging. *eNeuro*, *6*. **DOI:** https://doi.org/10.1523/ENEURO.0196-19.2019, **PMID:** 31772033, **PMCID:** PMC6924997
Sprague, T. C., Saproo, S., & Serences, J. T. (2015). Visual attention mitigates information loss in small- and large-scale neural codes. *Trends in Cognitive Sciences*, *19*, 215–226. **DOI:** https://doi.org/10.1016/j.tics.2015.02.005, **PMID:** 25769502, **PMCID:** PMC4532299
Sreenivasan, K. K., & D'Esposito, M. (2019). The what, where and how of delay activity. *Nature Reviews Neuroscience*, *20*, 466–481. **DOI:** https://doi.org/10.1038/s41583-019-0176-7, **PMID:** 31086326
Sutterer, D. W., Foster, J. J., Serences, J. T., Vogel, E. K., & Awh, E. (2019). Alpha-band oscillations track the retrieval of precise spatial representations from long-term memory. *Journal of Neurophysiology*, *122*, 539–551. **DOI:** https://doi.org/10.1152/jn.00268.2019, **PMID:** 31188708, **PMCID:** PMC6734397
Sutterer, D. W., Polyn, S., & Woodman, G. F. (2021). Alpha-band activity tracks a 2-dimensional spotlight of attention during spatial working memory maintenance. *Journal of Neurophysiology*, *125*, 957–971. **DOI:** https://doi.org/10.1152/jn.00582.2020, **PMID:** 33534657
Swets, J. A. (1961). Detection theory and psychophysics: A review. *Psychometrika*, *26*, 49–63. **DOI:** https://doi.org/10.1007/BF02289684
Thompson, T., Steffert, T., Ros, T., Leach, J., & Gruzelier, J. (2008). EEG applications for sport and performance. *Methods*, *45*, 279–288. **DOI:** https://doi.org/10.1016/j.ymeth.2008.07.006, **PMID:** 18682293
Thut, G., Nietzel, A., Brandt, S. A., & Pascual-Leone, A. (2006). α-Band electroencephalographic activity over occipital cortex indexes visuospatial attention bias and predicts visual target detection. *Journal of Neuroscience*, *26*, 9494–9502. **DOI:** https://doi.org/10.1523/JNEUROSCI.0875-06.2006, **PMID:** 16971533, **PMCID:** PMC6674607
van Moorselaar, D., Foster, J. J., Sutterer, D. W., Theeuwes, J., Olivers, C. N., & Awh, E. (2018). Spatially selective alpha oscillations reveal moment-by-moment trade-offs between working memory and attention. *Journal of Cognitive Neuroscience*, *30*, 256–266. **DOI:** https://doi.org/10.1162/jocn_a_01198, **PMID:** 29040014, **PMCID:** PMC6022736
Vogel, E. K., & Machizawa, M. G. (2004). Neural activity predicts individual differences in visual working memory capacity. *Nature*, *428*, 748–751. **DOI:** https://doi.org/10.1038/nature02447, **PMID:** 15085132
Vogel, E. K., McCollough, A. W., & Machizawa, M. G. (2005). Neural measures reveal individual differences in controlling access to working memory. *Nature*, *438*, 500–503. **DOI:** https://doi.org/10.1038/nature04171, **PMID:** 16306992
Wetzels, R., Matzke, D., Lee, M. D., Rouder, J. N., Iverson, G. J., & Wagenmakers, E. J. (2011). Statistical evidence in experimental psychology: An empirical comparison using 855 t tests. *Perspectives on Psychological Science*, *6*, 291–298. https://doi.org/10.117/1745691611406923. **DOI:** https://doi.org/10.1177/1745691611406923, **PMID:** 26168519
Wilken, P., & Ma, W. J. (2004). A detection theory account of change detection. *Journal of Vision*, *4*, 1120–1135. **DOI:** https://doi.org/10.1167/4.12.11, **PMID:** 15669916
Worden, M. S., Foxe, J. J., Wang, N., & Simpson, G. V. (2000). Anticipatory biasing of visuospatial attention indexed by retinotopically specific alpha-band electroencephalography increases over occipital cortex. *Journal of Neuroscience*, *20*, RC63. **DOI:** https://doi.org/10.1523/jneurosci.20-06-j0002.2000, **PMID:** 10704517, **PMCID:** PMC6772495
Yagi, Y., Coburn, K. L., Estes, K. M., & Arruda, J. E. (1999). Effects of aerobic exercise and gender on visual and auditory P300, reaction time, and accuracy. *European Journal of Applied Physiology and Occupational Physiology*, *80*, 402–408. **DOI:** https://doi.org/10.1007/s004210050611, **PMID:** 10502073
Zhang, W., & Luck, S. J. (2008). Discrete fixed-resolution representations in visual working memory. *Nature*, *453*, 233–235. **DOI:** https://doi.org/10.1038/nature06860, **PMID:** 18385672, **PMCID:** PMC2588137